Development and irradiation test of lost alpha detection system for ITER[a)]

M. Nishiura,[1,b)] T. Nagasaka,[1] K. Fujioka,[2] Y. Fujimoto,[2] T. Tanaka,[1] T. Ido,[1] S. Yamamoto,[3] S. Kashiwa,[4] and M. Sasao[4]
[1]*National Institute for Fusion Science, 322-6 Oroshi-cho, Toki 509-5292, Japan*
[2]*ILE, Osaka University, 2-6 Yamada oka, Suita 565-0871, Japan*
[3]*Kyoto University, Gokasho Uji, Kyoto 611-0011, Japan*
[4]*Tohoku University, Aoba 6-01-2, Sendai 980-8579, Japan*

(Presented 17 May 2010; received 17 May 2010; accepted 27 July 2010; published online 19 October 2010)

We developed a lost alpha detection system to use in burning plasma experiments. The scintillators of Ag:ZnS and polycrystalline Ce:YAG were designed for a high-temperature environment, and the optical transmission line was designed to transmit from the scintillator to the port plug. The required optical components of lenses and mirrors were irradiated using the fission reactor with the initial result that there was no clear change after the irradiation with a neutron flux of 9.6×10^{17} nm^{-2} s^{-1} for 48 h. We propose a diagnostic of alpha particle loss, so-called alpha particle induced gamma ray spectroscopy. The initial laboratory test has been carried out by the use of the Ce doped Lu_2SiO_5 scintillator detector and an Am–Be source to detect the 4.44 MeV high energy gamma ray due to the $^9Be(\alpha,n\gamma)^{12}C$ reaction. © *2010 American Institute of Physics.*
[doi:10.1063/1.3485118]

I. INTRODUCTION

Two types of alpha particle loss diagnostic system are proposed for burning plasma experiments such as those at International Thermonuclear Experimental Reactor (ITER). The first system is based on the conventional scintillator lost ion probes, which can detect the lost fast ions escaping to the first walls with a gyration motion. From the information on the scintillator image, the energy and pitch angle distributions of fast ions can be obtained simultaneously. The loss location of alpha particles and fast ions is localized on the first walls, allowing investigation of the detector location using ion-orbit calculations.[1] Funaki *et al.* proposed the modification of first wall shapes to collect MeV alpha particles.

The endurance and the light output under ITER environments have been studied by MeV ion beam and γ-ray irradiation. The linearity and the endurance of light output for polycrystalline Ce doped $Y_3Al_5O_{12}$ (Ce:YAG) for proton[2] and helium beams[3] with MeV energies have been reported previously. The radiation damage by irradiation using a nuclear reactor and the characteristics of recovering light output by annealing are also described in Ref. 3. Following the 2007 Large Helical Device (LHD) plasma experimental campaign, the scintillator of the lost ion probe for the LHD is changed by replacing Ag:ZnS with the polycrystalline transparent Ce:YAG ceramics. The LHD experiments can test the high-temperature use without neutrons and γ-rays. The lost ion probe, in which the Ce:YAG scintillator is mounted, has been demonstrated for the measurement of fast ion loss signals under ~200 °C.

The total system of a lost alpha detector is considered in this paper. Scintillation light must be transmitted efficiently from the head location of the lost alpha detector mounted inside first walls of ITER. For this system, the radiation hardness of optical components is tested.

A second new system is based on the $^9Be(\alpha,n\gamma)^{12}C$ reaction at first wall, which is applied to the alpha particle induced γ-ray detection.[4,5] The energy resolution of Ce doped Lu_2SiO_5 (Ce:LSO) (Ref. 6) is not characterized adequately for our purpose. We investigated the energy resolution of Ce:LSO for a peak of 4.44 MeV gamma ray as one of the possible scintillator detectors. Using the results of our investigation, we discuss the issues for the signal-to-noise (S/N) ratio and the pile-up.

II. LIGHT OUTPUT OF SCINTILLATORS FOR ION IRRADIATION UNDER HIGH-TEMPERATURE ENVIRONMENTS

The blanket modules for ITER, where a lost alpha detector is mounted, are operated at the temperature of around 300 °C. In the most severe case, it may heat up to about 1000 °C, which is a transient phenomenon such as a disruption. Therefore even if the temperature is heated up to 1000 °C, the scintillator can emit the light at ~300 °C again after cooling. Heat resistance and light output at high temperature are required for the phosphors. We prepared two specimen of Ag:ZnS and Ce:YAG for ion beam irradiation experiments. The former sample was the Ag:ZnS powder (P11, Sylvania) pasted on a quartz plate. A transparent polycrystalline Ce:YAG fabricated from raw materials and sin-

[a)]Contributed paper, published as part of the Proceedings of the 18th Topical Conference on High-Temperature Plasma Diagnostics, Wildwood, New Jersey, May 2010.
[b)]Author to whom correspondence should be addressed. Electronic mail: nishiura@nifs.ac.jp.

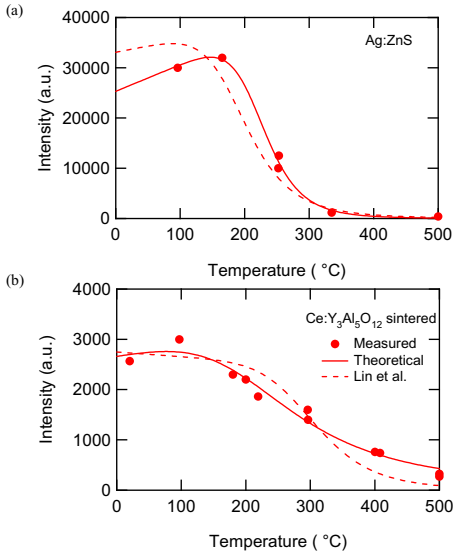

FIG. 1. (Color online) Characteristics of light output on scintillator temperature (a) Ag:ZnS and (b) Ce:YAG. The solid curve is the theoretical fitting. The dotted one is the theoretical fitting by Lin *et al.* (Ref. 7).

tered at a temperature of 1750 °C. The 1 mol % cerium was doped in YAG. All processes for Ce:YAG are consolidated at the Institute of Laser Engineering at Osaka University.

The MeV ion beam was irradiated onto two scintillators at the accelerator facility of the Fast Neutron Laboratory (FNL) at Tohoku University. Each specimen was attached tightly on the sample holder with heat control in a vacuum chamber. The specimen was heated to 500 °C initially and the temperature was then decreased to room temperature. The spectrum intensity in the range from 450 to 800 nm was measured by a spectrometer (Hamamatsu, PMA11), while the ion beam was irradiated onto the scintillator.

The measured spectrums of Ag:ZnS and Ce:YAG had peaks at 420 and 560 nm, respectively. The light output at peak intensity is plotted as a function of the scintillator temperature in Fig. 1(a) for Ag:ZnS and Fig. 1(b) for Ce:YAG. The H^+ beam with 3 MeV energy is irradiated at the beam current of 36–38.5 nA for Ag:ZnS and at 4.1–4.8 nA for Ce:YAG. The light output at more than 200 °C decreases and quenches at 500 °C for Ag:ZnS. The polycrystalline Ce:YAG emits a higher light output than Ag:ZnS at 500 °C, when the measured light output is normalized by the irradiated beam current. The result is better performance for a lost alpha detector under a high temperature environment. The theoretical curves derived by Lin *et al.*[7] are plotted as dotted lines, and our theoretical curves are plotted as solid lines. The fitting parameters by Lin *et al.* are slightly different from ours for both materials. This would be caused by the materials, the impurity contamination, dopant density, grain size, transparency, and so on.

The spectrums for Ce:YAG are plotted in Fig. 2 with temperature from 200 to 500 °C. The same data in Fig. 1(b) are used. The wavelength at the maximum light output shifts from 572 to 595 nm, as the temperature rise from 200 to 500 °C. The heat radiation from the back plate heater is observed at the wavelength of more than 800 nm only in the

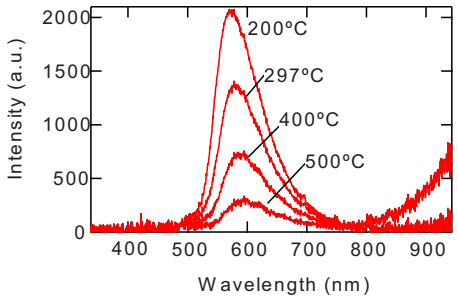

FIG. 2. (Color online) Dependence of light output on Ce:YAG temperature. The H^+ beam irradiated onto Ce:YAG is in Fig. 1(b). At 500 °C, a thermal radiation from the heater is observed at more than 800 nm.

case of 500 °C. The heat radiation that may interfere the scintillator light is removed by using a low pass filter.

The decay time of 88 ns is obtained for Ce:YAG excited by a pulse Nd:YAG laser at 355 nm wavelength. This time response is good resolution to measure plasma instabilities such as Alfvén activities in burning plasmas.

III. DEMONSTRATION OF LARGE TRANSPARENT CERAMICS

We sintered the large size of transparent polycrystalline Ce:YAG for the LHD scintillator lost ion probe (LHD-SLIP) and were able to fabricate a diameter of 40 mm and a thickness of 1 mm. Three samples were prepared to optimize the doped Ce density. The light output of Ce:YAG for 0.4, 0.55, and 1.0 mol % was measured, and that of 0.4 mol % decreased to 0.8 of that of the other samples. Therefore we selected the 0.55 mol % Ce:YAG for LHD-SLIP. Figure 3 shows the Ce:YAG scintillator mounted inside the molybdenum probe head of LHD-SLIP. The probe head was attached to the tip of the periscope cylinder. When the LHD-SLIP was located near the plasma boundary, the scintillator temperature was increased from room temperature to ~300 °C and was piled up during plasma discharges.

In the LHD discharge, fast ion losses are measured using the Ce:YAG scintillator. The SLIP is installed from the upper port of the LHD. Figure 4 shows the typical result of fast ion losses during neutral beam (NB) injection. The pitch angle and the energy of fast ions are measured by an image-

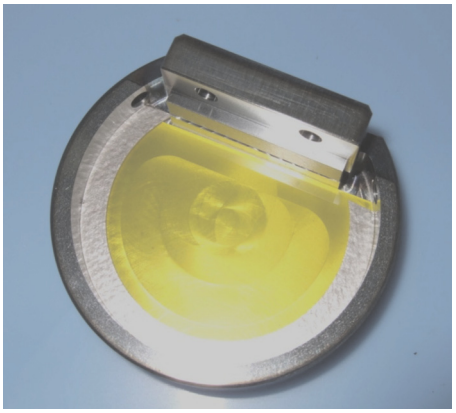

FIG. 3. (Color online) Polycrystalline transparent Ce:YAG scintillator mounted to the molybdenum probe head of a LHD scintillator lost ion probe.

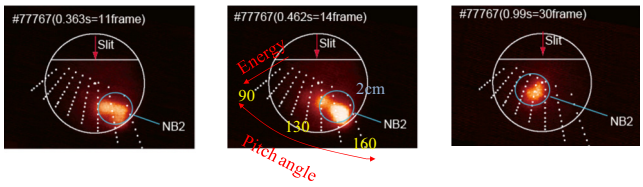

FIG. 4. (Color online) Temporal behavior of fast ion losses during NB no. 2 heating in LHD discharge. The images correspond to t=0.363, 0.462, and 0.990 s, respectively.

intensified charge-coupled device (CCD) camera. The grid for the pitch angle from 90° to 160° and the gyroradius from 2 cm with 1 cm increments is superimposed on the camera image. The fast ions are produced by the counter NB no. 2, and the pitch angle of lost fast ions changes from the pitch angle of 150° to 120° with the growth of plasmas. The electron density and the electron temperature were 0.5–1 $\times 10^{19}$ m^{-3} and 1–2 keV, respectively.

IV. DESIGN OF LIGHT TRANSMISSION LINE

The scintillation light is transmitted from a probe head to outside of a vacuum vessel. When the probe head is mounted inside a blanket module, the optical transmission line from the probe head is connected to a port plug through blanket and blanket shield modules. For the ITER lost alpha detector, we designed the optical transmission line by utilizing a relay lens system. The long optical transmission is similar to the LHD probe system, which has the distance of 5.2 m between the scintillator and the vacuum seal window. We adopt this LHD relay lens system for the ITER lost alpha detector, which has the distance of ~2.7 m between the scintillator mounted on the blanket module no. 16 and the port plug.

The lens diameter is limited to 30 mm. The mirrors are used for bending the light direction. The design parameters are summarized in Table I, and the schematic drawing is shown in Fig. 5. The design of the optical transmission line consists of 16 lenses and five mirrors. Since the transmission line in the port plug is not treated here, the total number of optical components is actually more than these numbers. The final optics of the relay lens system is connected to the fiber bundle coupled with an image-intensified CCD camera and/or a photomultiplier array. Further investigation of the optics design is required, based on the irradiation data for fibers and quartz.[8,9]

TABLE I. Design parameters of the lost alpha detection system for ITER.

Composition	Relay lens system
Wavelength	500 nm$<\lambda<$700 nm (main wavelength 550 nm)
Object	Scintillator ϕ 30 mm
Image size	ϕ 6.0 mm
Image magnification	6/30=0.2
Image effective F number	3.6 (numerical aperature 0.14)
Scintillator-port plug	2680.4 mm

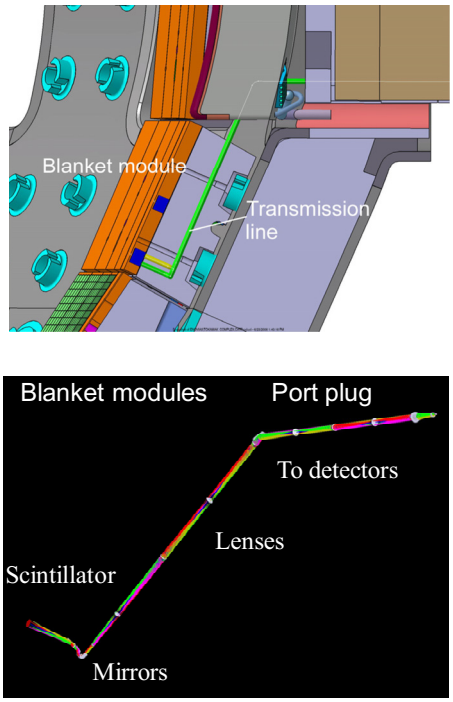

FIG. 5. (Color online) Side view of the blanket module no. 16 in ITER. Design of the light transmission line of the lost alpha detector. The design parameters are listed in Table I.

V. RADIATION HARDNESS OF OPTICAL COMPONENTS

The optical components require radiation hardness in burning plasma experiments on ITER and other fusion devices. The irradiation test for these components is performed using a nuclear reactor (JRR-3). The thermal neutron flux of 9.6×10^{17} n/m^2 s and the fluence of 1.7×10^{23} n/m^2 for 48 h are irradiated using the rabbit method of the JRR-3 reactor. The fast neutron flux is about one order of magnitude lower than the thermal one. The irradiation of neutron and gamma ray deteriorates the light output of ~30% of no irradiated Ce:YAG.[3] The Ce:YAG is pale brown after irradiation. The transmittance of Ce:YAG for 48 h rabbit irradiation is worse at wavelengths less than 400 nm than that with no irradiation because a defect (color center) is created and it interferes with the light emission. The quartz lenses and the Al-coated mirrors on the quartz substrates are also irradiated under the same conditions as described above. No clear change can be discerned. The reflectance and the transmittance for lenses and mirrors will be characterized in the near future.

VI. S/N RATIO FOR ALPHA PARTICLE DETECTION

When the Ce:YAG scintillator is located near the first wall, the S/N ratio can be estimated for lost alpha particle detection. The alpha particles with the energy of ~3.5 MeV, which hit the Ce:YAG scintillator directly, are detected effectively, while the sensitivity for the background γ-rays and neutrons must be reduced as much as possible. The simple one-dimensional model is employed for two cases (the Ce:YAG thickness of 1 and 0.01 mm). The fluxes of alpha particles, γ-rays, and neutrons are set to 1×10^{17} ions/m^2 s, 2×10^3 Gy/s at Fe, and 3×10^{18} n/m^2 s, respectively, from

the thickness direction for the input parameters of the MCNP code.[10] The argument for these values is difficult, but the flux of alpha particles is based on the extrapolation from the reference[11] of deuterium tritium (DT) operation at TFTR. If we use the heat flux of 50 kW/m^2 calculated by ASCOT code,[12] the particle flux with energy of 3.5 MeV is of the order of about 10^{17} alpha/m^2 s. However since the alpha particle has prompt and slowing down losses and the losses are not uniform on the first walls, the S/N ratio goes up/down as the flux may decrease/increase. The neutron flux near the blanket module is calculated by MCNP code with Alite model version 4 of ITER assuming the fusion output power of 400 MW during the operation scenario two. The result shows the same order of magnitude for the neutron flux of $\sim 10^{18}$ n/m^2 s (Ref. 13) near the first wall surface. The thickness of 1 mm Ce:YAG is the S/N ratio of 0.65. When the thickness is reduced to 0.01 mm for the better S/N ratio, which is still longer than the alpha particle range in Ce:YAG, the S/N ratio is about 65. The S/N ratio would be worse because the degradation by radiations, the optical transmission loss, and the neutron noise scattered from the circumference are not included in the calculation.

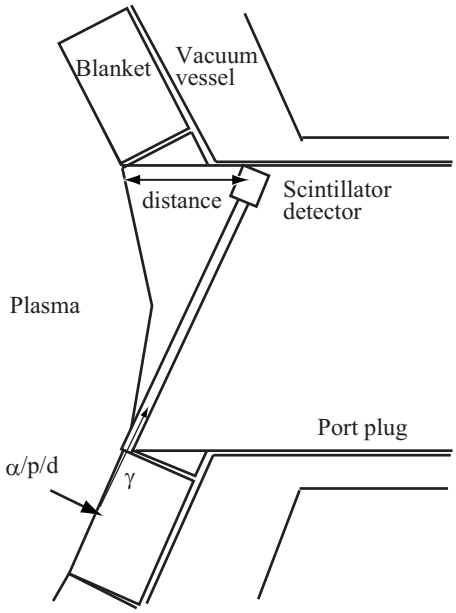

FIG. 6. Concept of alpha particle (ion) induced gamma ray spectroscopy. Scintillator detector is located in the port plug of ITER, and the sightline is directed to the first wall.

VII. LOST ALPHA (ION) INDUCED GAMMA RAY SPECTROSCOPY

In addition to the conventional detection of alpha particle and fast ion losses, we considered the method utilizing the nuclear reactions at the first walls of ITER. The alpha particle losses onto the first wall surface create neutrons and γ-rays due to the $^9Be(\alpha,n\gamma)^{12}C$ reaction, because the ITER first wall is made of beryllium metal. The γ-ray detection may allow us to measure the alpha particle losses onto the first walls. The 4.44 MeV γ-rays from the $^9Be(\alpha,n\gamma)^{12}C$ reaction must be discriminated from the background γ-rays and neutrons originating from DT plasmas, vacuum vessel, and first walls. Even in the deuterium deuterium (DD) discharge, the 3.1 MeV γ-rays from the reaction $^{12}C(d,p\gamma)^{13}C$ is possible. The reaction has already utilized successfully for the confined alpha and ion diagnostics in DT and DD plasmas of JET.[5]

We consider that the line of sight is directed to the first walls, where the charged fusion products hit, but is not directed to the plasmas for the background neutron and gamma reduction, as shown in Fig. 6. There are some merits to simplifying the conventional lost alpha detection system. When the scintillator is located in a port plug, it does not depend on the shape of a detector head, and no modification of blanket modules occurs. It covers all areas, where we want to diagnose the loss location, by arranging the detector position. It avoids the hard irradiation of optical components. It leads to longer lifetimes of these components. However, this diagnostic system suffers from the background level of neutrons and γ-rays. The S/N ratio should be evaluated by MCNP code with DT operation of ITER to validate the 4.4 MeV γ-ray detection. The hollow flight tube on the sightline is illustrated in Fig. 6 for diagnosing the blanket module no. 16. The scintillator detector is located at the distance of 0.8 m from the first wall, and is exposed to the total neutron and γ fluxes, which are $\sim 10^{16}$ n/m^2 s and 3×10^{15} γ/m^2 s, respectively. Further developments for a sightline, a background radiation shield, and a total diagnostic system are still needed to obtain efficient S/N ratios. As a first step, the next section shows the feasibility test of 4.44 MeV γ-ray detection using an inorganic scintillator.

VIII. LABOTATORY TEST OF LOST ALPHA (ION)-INDUCED γ-RAY SPECTROSCOPY

For the demonstration of lost alpha-induced γ-ray spectroscopy, we utilized an Am–Be source to simulate the alpha particle losses onto the first wall surface of beryllium in ITER. The Am–Be source produces 4.4 MeV γ-rays as well as neutrons from the $^9Be(\alpha,n\gamma)^{12}C$ reaction, and it emits the neutrons of 2.3×10^4 n/s and γ-rays of 1.4×10^4 γ/s. The spectrum of high-energy γ-rays is obtained by a pulse height analysis. The 0.1 mol % Ce:LSO scintillator ($10\times 10\times 20$ mm) is selected because of the inclusion of the heavy element. Teflon tape covers five faces of the Ce:LSO scintillator for the reflection of light. The Ce:LSO scintillator is directly coupled with a photomultiplier. Silicon grease is pasted in between the incident window and Ce:LSO scintillator for efficient coupling. The photomultiplier (Hamamatsu, H3178–61) is biased at the voltage of -650 V, and the output signal is connected to the preamplifier and to the shaping amplifier (ORTEC, 570). The energy spectrum is obtained by a multichannel analyzer (ORTEC, MCA7600).

Figure 7 shows the γ-ray spectrum using the LSO scintillator. The γ-rays are irradiated onto a 20 mm$\times$10 mm portion of the face of the LSO scintillator. The full energy peak of 4.44 MeV γ-rays, plus single escape, and double escape peaks are clearly distinguished. The energy resolution of 6.2 % is obtained at 4.44 MeV full-energy peak. The synthetic spectrum calculated by EGS4 (electromagnetic Monte Carlo code)[14] is plotted in the same figure. The cal-

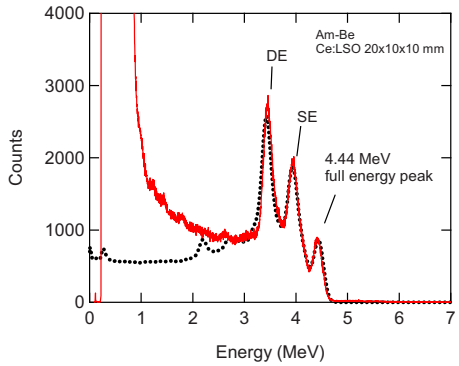

FIG. 7. (Color online) γ-ray spectrum by LSO scintillator. DE: double escape peak, and SE: single escape peak. The dotted line is the synthetic γ-ray spectrum calculated by EGS4.

culated spectrum is convoluted with the experimental resolution of 6%. The vertical axis is scaled by the measured counts at the full energy peak. The calculated spectrum is in good agreement with the experimental one in the energy range of more than 3 MeV, while the lower energy region has a discrepancy. This is due to the self-decay process of ^{176}Lu in LSO itself. From the result, LSO is found to be an efficient scintillator for 4.44 MeV γ-rays. EGS4 simulation is useful for designing and optimizing the γ-ray detection system.

In the cases of a ^{137}Cs and ^{60}Co sources, the energy resolution of 12.9% is obtained at 662 keV for the ^{137}Cs source, 7.9% at 1.17 MeV and 9.5% at 1.33 MeV for the ^{60}Co source, respectively.

The decay time of 50 ns is obtained for Ce:LSO excited by a pulse Nd:YAG laser at 355 nm wavelength in the same method for Ce:YAG. The light output and decay time for Ce:LSO should be characterized for the use of high temperature around 300–500 °C.

ACKNOWLEDGMENTS

This work was supported by a Grant-in-Aid from the Ministry of Education, Culture, Sports, Science, and Technology of Japan, "Priority Area of Advanced Burning Plasma Diagnostics." We thank the LHD experiment group, the ITER CAD team, FNL, Oarai Branch of Institute for Materials Research, and the Cyclotron facility at Tohoku University for their support.

[1] D. Funaki, M. Isobe, M. Nishiura, Y. Sato, A. Okamoto, T. Kobuchi, S. Kitajima, and M. Sasao, Rev. Sci. Instrum. **79**, 10E512 (2008).
[2] M. Nishiura, N. Kubo, T. Hirouchi, T. Ido, T. Nagasaka, T. Mutoh, S. Matsuyama, M. Isobe, A. Okamoto, K. Shinto, S. Kitajima, M. Sasao, M. Nakatsuka, and K. Fujioka, Rev. Sci. Instrum. **77**, 10E720 (2006).
[3] T. Hirouchi, M. Nishiura, T. Nagasaka, T. Ido, M. Sasao, K. Fujioka, M. Isobe, and T. Mutoh, J. Nucl. Mater. **386–388**, 1049 (2009).
[4] G. Bonheure and G. Van Wassenhove, Rev. Sci. Instrum. **74**, 1726 (2003).
[5] V. G. Kiptily, F. E. Cecil, and S. S. Medley, Plasma Phys. Controlled Fusion **48**, R59 (2006).
[6] M. Moszynski, M. Balcerzyk, M. Kapusta, D. Wolski, and C. L. Melcher, IEEE Trans. Nucl. Sci. **47**, 1324 (2000).
[7] Z. Lin, R. L. Boivin, and S. J. Zweben, Princeton Plasma Physics Laboratory Report No. PPPL-TM-392, 1992.
[8] T. Shikama, T. Kakuta, N. Shamoto, M. Narui, and T. Sagawa, Fusion Eng. Des. **51–52**, 179 (2000).
[9] T. Kakuta, T. Shikama, T. Nishitani, B. Brichard, A. Krassilinikov, A. Tomashuk, S. Yamamoto, and S. Kasai, J. Nucl. Mater. **307–311**, 1277 (2002).
[10] J. F. Briesmeister, "MCNP-A general Monte Carlo *N* -particle transport code version 4C," Los Alamos National Laboratory Report No. LA-13709-M, 2000.
[11] M. Tuszewski and S. J. Zweben, Rev. Sci. Instrum. **64**, 2459 (1993).
[12] T. Kurki-Suonio, O. Asunta, T. Hellsten, V. Hynönen, T. Johnson, T. Koskela, J. Lönnroth, V. Parail, M. Roccella, G. Saibene, A. Salmi, and S. Sipilä, Nucl. Fusion **49**, 095001 (2009).
[13] G. Vayakis, E. R. Hodgson, V. Voitsenya, and C. I. Walker, Fusion Sci. Technol. **53**, 699 (2008).
[14] Y. Namito, S. Ban, and H. Hirayama, Nucl. Instrum. Methods **349**, 489 (1994).